Bone 195 (2025) 117466

Contents lists available at ScienceDirect

Bone

journal homepage: www.elsevier.com/locate/bone

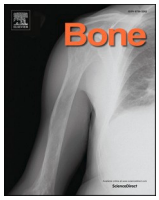

Full Length Article

Extracellular pH is a critical regulator of osteoclast fusion, size and activation

Bethan K. Davies [a,b], Andrew J. Skelton [c], Mark Hopkinson [a], Simon Lumb [c], Gill Holdsworth [c], Timothy R. Arnett [d], Isabel R. Orriss [a,*]

[a] Department of Comparative Biomedical Sciences, Royal Veterinary College, London, UK
[b] Department of Chronic Diseases and Metabolism, KU Leuven, Belgium
[c] UCB Pharma Ltd., Slough, UK
[d] Department of Cell and Developmental Biology, University College London, London, UK

ARTICLE INFO

Keywords:
Osteoclast
Formation
Fusion
Resorption
Acidosis

ABSTRACT

Osteoclast activity is regulated by extracellular pH, whereby bone resorption is near-maximally activated at pH 7.0 but limited at ≥pH 7.4. This study examined the effects of low pH on osteoclast fusion, multi-nucleation, resorption and cell transcriptome. Osteoclasts were cultured on dentine discs at pH 7.4 (control) or pH 7.0 (acidified) for 5–7 days. Osteoclast number and resorptive activity were 1.9-fold and 6.7-fold higher, respectively, in acidified cultures. However, acidified osteoclasts were smaller, with fewer nuclei than controls (53 μm diameter with 9 ± 1 nuclei/cell versus 100 μm with 24 ± 3 nuclei/cell). mRNA expression analysis revealed that osteoclast formation and resorption-associated genes were increased in acidified osteoclasts. Switching mature osteoclasts formed for 5 days at pH 7.4 to acidified conditions decreased cell size 30 % within 4 h, resulting in a 2-fold increase in osteoclast numbers after 24 h. Resorptive activity in cells switched to pH 7.0 was visible within 8 h, and by 24 h resorption area was comparable to continually acidified osteoclasts. MicroCT analysis of dentine discs revealed 24-fold and 6.4-fold increases in resorption pit number in pH-switched osteoclasts relative to control and acidified cultures, respectively. RNAseq showed changes in extracellular pH differentially regulated gene expression, particularly metabolic and cell cycle-associated genes. Our results reveal previously unknown effects of extracellular pH on osteoclasts. Specifically, they show pH is an important modulator of osteoclast fusion and size that regulates the transcriptome. Furthermore, small changes in pH can induce significant morphological changes in osteoclasts and act as on/off switch between formation and resorption in ≤4 h.

1. Introduction

Osteoclasts, the bone resorbing cell, are multinucleated cells of haematopoietic origin that form by the fusion of monocyte/macrophage precursors. Osteoclast formation is a complex, multi-step process that requires macrophage-colony stimulating factor (M-CSF), receptor activator of nuclear factor κ-B ligand (RANKL) and nuclear factor of activated T-cells, cytoplasmic 1 (Nfatc1) for precursor proliferation and commitment, respectively [1–3]. Mononuclear pre-osteoclasts fuse at the bone surface to form multinuclear, mature functional osteoclasts in a process that is not fully understood. Osteoclast fusion is facilitated by many factors including dendritic cell-specific transmembrane protein (DC-STAMP), osteoclast stimulatory transmembrane protein (OC-STAMP), the vacuolar H^+-ATPase (vATPase) subunit ATPv60d2, syncytin-B and CD47 [4–8]. To resorb, osteoclasts undergo morphological and ultrastructural changes, principally polarisation, through sealing zone and ruffled border formation. Osteoclast polarisation upregulates resorption-associated genes (e.g., carbonic anhydrase II (CAII) and vATPase) [9,10]. Proton (H^+) and chloride (Cl^-) ions are subsequently pumped into the resorption lacunae through the ruffled border to dissolve the hydroxyapatite mineral. The demineralised bone matrix is then degraded by proteases including cathepsin K, matrix metalloproteinases (MMPs) and tartrate resistant acid phosphatase (TRAP).

Systemic acidosis occurs through the dysregulation of the acid-base balance and its profound negative effect on the skeleton is well-characterised [11]. To buffer excess H^+ concentrations under acidosis, alkaline material, specifically calcium carbonate, is released from bone

* Corresponding author at: Department of Comparative Biomedical Sciences, Royal Veterinary College, Royal College Street, London NW1 0TU, UK.
E-mail address: iorriss@rvc.ac.uk (I.R. Orriss).

https://doi.org/10.1016/j.bone.2025.117466
Received 22 November 2024; Received in revised form 14 March 2025; Accepted 18 March 2025
Available online 20 March 2025

[11,12]. Early studies showed that calcium release from live bones was consistent over a physiological pH range (pH 7.03–7.49) but was inhibited at extreme pH (<6.8 or > 7.4) [13]. This, and other work, concluded that acidosis can indirectly stimulate bone resorption by physicochemical dissolution of bone mineral [14]. Other studies, however, showed that parathyroid hormone amplified calcium release, whereas sodium azide (a metabolic inhibitor) inhibited it, implying that mechanisms other than mineral dissolution are involved [15].

The first direct demonstration that osteoclast activity is modulated by protons was by Arnett and Dempster [16]. This and subsequent studies have shown that a step-wise reduction in medium pH between pH 7.4 and pH 6.8 produces a graded increase in resorption area and pit number, depth and width [16–18]. Little or no resorption occurs at a neutral pH (pH 7.4), whereas resorption increases significantly as the pH becomes more acidic. Specifically, osteoclast activity is up to 5-, 9- and 14-fold higher at pH 7.2, 7.0 and 6.8, respectively [16–18]. In fact, resorption pit formation increased 6-fold over pH 7.25 and 7.15, demonstrating that even small changes in pH sensitively modulate osteoclast function [18]. Studies in mouse calvariae cultured in HCl-acidified media similarly report dose-dependent increases in calcium release [19,20]. This H^+-induced calcium release was blocked by indomethacin, a prostaglandin inhibitor, and calcitonin, reinforcing the cellular component in bone resorption [19,20]. The acid sensitivity of osteoclast-mediated bone resorption has now been reported in rodent, chick, rabbit, and feline osteoclasts [16,19,21–23].

Acidosis also promotes intracellular and cytoskeletal changes in osteoclasts. For example, acid pH induces TRAP, cathepsin K and CAII mRNA expression for subsequent resorptive function [9]. Similarly, extracellular acidification of osteoclasts to pH 7.0 decreases intracellular pH and Ca^{2+} concentrations and increases sealing zone formation for attachment to the bone matrix [21]. Conversely, alkalinisation of osteoclasts curtailed sealing zone formation [21,24]. Together, these data indicate that pH regulates the “off/on switch” for osteoclast activity.

The role of extracellular pH on osteoclast formation and fusion, however, is less well-characterised. In a co-culture system of an osteoblast-like cell line and osteoclasts, physiologically low pH (6.8–7.0) was reported to increase the formation of larger, more numerous osteoclasts, whereas pH 7.4 inhibited osteoclast formation [25,26]. However, a preliminary investigation in our laboratory using purified osteoclast-forming mouse marrow cultures on dentine suggested the opposite result [27]. The aim of the present study was, therefore, to characterise in vitro the direct actions of low pH on the formation, fusion, and function of osteoclasts.

2. Methods

2.1. Reagents

All tissue culture reagents were purchased from Life Technologies (Paisley, UK) and chemical reagents were purchased from Sigma-Aldrich (Poole, UK), unless otherwise stated.

2.2. Animals

C57BL/6 J mice (Charles River, UK) were group housed under standard conditions with free access to food and water. All animal procedures complied with the UK Animals (Scientific Procedures) Act 1986 and were reviewed and approved by the Royal Veterinary College Research Ethics Committee.

2.3. Osteoclast formation and resorption cultures

Osteoclast precursor cells were isolated from the long bones of ≥6-week-old male and female mice in combination as previously described [27]. For RNA sequencing (RNAseq), osteoclasts from 7-week-old female mice were used. Basal cell culture medium was Minimum Essential Medium supplemented with 10 % FCS, 2 mM L-glutamine, 100 U/ml penicillin, 100 μg/ml streptomycin and 0.25 μg/ml amphotericin (complete mixture abbreviated to MEM). All osteoclast cultures were performed using the same batch of FBS. In a 96-well tray, cells were seeded onto 5 mm dentine discs (10^6 cells/disc) in MEM supplemented with 100 nM PGE_2, 200 ng/ml M-CSF and 5 ng/ml RANKL (R&D Systems Ltd., Abingdon, UK). After 24 h, discs containing adherent osteoclast precursors were transferred to 6-well trays (4 discs/well in 4 ml medium) and supplemented with 10MEq/l NaOH or 10MEq/l HCl to achieve a media pH of pH 7.4 (control) and pH 7.0 (acidified), respectively. Cultures were terminated after 5–6 days.

To observe the effects of short-term acidification on osteoclasts, day 5 osteoclasts cultured at pH 7.4 and pH 7.0 were completely media changed. An additional pH 7.4 treatment group was acidified to pH 7.0 through 10Meq/l HCl addition. Cultures were terminated 0-, 4-, 8- and 24-h post-acidification unless otherwise stated. Herein, cells continually cultured at pH 7.4 and pH 7.0 will be referred to as ‘control’ and ‘acidified’ osteoclasts, respectively. Osteoclasts changed from control to acidified pH for the final 4–24 h of culture are termed ‘switched’. A schematic of the experimental set up is also shown in Fig. 4F. In all experiments, the pH of culture media was measured at the end of the experiment using the VetScan® i-STAT® 1 (ABAXIS, UK), a clinically used system that measures pCO_2, pO_2, HCO_3^- as well pH.

Dentine discs with adherent osteoclasts were fixed in 2.5 % glutaraldehyde, stained for tartrate-resistant acid phosphatase (TRAP) activity and imaged by reflective light microscopy using a DM400B upright microscope (Leica Microsystems, UK). Osteoclast number and the area resorbed per osteoclast (using a 16 × 12 grid overlay) were blindly assessed by dot-counting morphometry using ImageJ, as previously described [28]. Osteoclast diameter was also measured using ImageJ.

2.4. Immunofluorescence

Control and acidic osteoclasts cultured on dentine discs were fixed with 4 % paraformaldehyde in PBS for 20 min at room temperature and stored at 4 °C in PBS until staining. Osteoclasts were permeabilised in 0.2 % Triton-X for 5 min. Discs were washed 3 × 5 min in PBS. Cells were blocked in 4 % BSA in PBS for 30 min and washed 3 × 5 min in PBS. Discs were incubated for 1 h with 1:400 phalloidin Alexa 633 in PBS to stain for F-actin (excitation: 632 nm, emission: 647 nm). After three 5-min PBS washes, discs were mounted onto microscope slides using DAPI (excitation: 350 nm, emission: 470 nm) and viewed using a DM4000B fluorescence microscope (Leica Microsystems, UK). The number of nuclei per osteoclast was manually quantified using ImageJ.

2.5. Cell viability assay

Cell viability was determined using the CytoTox 96® Non-Radioactive Cytotoxicity Assay (Promega, UK), as per the manufacturer's instructions. Cytotoxicity was measured in control, acidified and switched osteoclasts. Briefly, cell supernatants were collected to determine medium LDH levels prior to cell lysis in 10 % (v/v) Triton® X-100 in water. After a 45-min incubation at 37 °C, a second supernatant sample was taken. The LDH content of the supernatant and cell lysates were measured spectrophotometrically (490 nm), as per the manufacturer's instructions. A negative control was pH-adjusted media that had not been exposed to cells; a 1:5000 dilution of bovine heart LDH acted as positive control. Cell viability was calculated by expressing medium LDH as a percentage of the total cellular LDH.

2.6. Total RNA extraction

Control and acidified osteoclasts were cultured on dentine discs for 5 days before being transferred to a new plate to ensure that only RNA from dentine-associated osteoclasts was isolated. For RNAseq, total RNA was isolated from control, acidified and switched osteoclasts 4-h post-

acidification. Osteoclast RNA was collected using Qiazol® reagent (Qiagen Ltd., UK). Lysates were stored at -80 °C until required. Total RNA was extracted using the miRNEasy® Mini kit (Qiagen, UK) as per the manufacturer's instructions. Total RNA was quantified spectrophotometrically by measuring absorbance at 260 nm (NanoDrop 1000). RNA was stored at -80 °C until needed.

2.7. Real-time quantitative polymerase chain reaction (RT-qPCR)

Osteoclast RNA (50 ng/μl) was simultaneously reverse-transcribed and amplified using the qPCRBIO SyGreen 1-step Go Lo-Rox qPCR kit (PCR Biosystems, UK), according to manufacturer instructions. Reactions were performed in a BioRad Connect CFX thermocycler (BioRad, UK) with initial cDNA synthesis (45 °C, 10 min), reverse transcriptase inactivation and polymerase activation (95 °C, 2 min) followed by 40 cycles of denaturation (95 °C, 5 s) and primer annealing, extension of DNA and detection (60 °C, 30 s). Primer sequences are shown in Table 1. All reactions were carried out in triplicate using RNAs derived from 5 different osteoclast cultures. Data were normalised to TATA-binding protein (TBP) and analysed using the ΔΔCt method [29].

2.8. Western blotting

Protein was extracted from control and acidified osteoclasts cultured for 5 days. Cells on dentine discs were transferred to a new plate, lysed in ice-cold radio immunoprecipitation (RIPA) buffer, sonicated for 5 min and homogenates were stored at -80 °C until use. Lysate protein concentrations were measured using the Bradford assay (BioRad, UK). Protein samples were incubated with 5× reducing sample buffer and denatured at 100 °C for 5 min prior to loading onto 4–20 % Tris-HCl sodium dodecyl sulfate-polyacrylamide gel electrophoresis gels (4–16.5 μg/lane). Gels were run in a wet tank blotter (BioRad, UK) prior to transfer to an Amersham™ polyvinylidene fluoride (PVDF) membrane (GE Healthcare, UK). Membranes were blocked with 5 % non-fat milk and incubated with β-actin (1:5000, ProteinTech, 20,536–1-AP), DC-STAMP (1:500, Sigma-Aldrich, MABF39-I), CAII (1:500, ProteinTech, 16,969–1-AP), cathepsin K (1:300, ProteinTech, 11,239–1-AP) and OPN (1:1000, Abcam, Ab283656) antibodies overnight at 4 °C. After washing in 0.05 % Tween-PBS, blots were incubated at room temperature for 1 h with horseradish peroxidase-conjugated secondary antibodies (Jackson ImmunoResearch, UK). A peroxidase detection system (Immobilon™ Western, Merck-Millipore) and ChemiDoc™ XRS+ system (BioRad, UK) was used to visualise blot immunoreactivity. Developed blots were quantified using ImageJ.

Table 1
Primer sequences.

Gene name	Primer sequence (5′ to 3′)
Tbp	For: GGCGGTTTGGCTAGGTTT
	Rev: TCTGGGTTATCTTCACACACCA
Tnfrsf11a (RANK)	For: GGGTGATTTTCTTTTGGTGGGTC
	Rev: TGCTCGTGATAACTATGCCTGTGG
Csf1r	For: GATGTGTGAGCAATGGCAGTGTG
	Rev: TCAGGGTCCAAGGTCCAGTAGG
Nfatc1	For: TCATCCTGTCCAACACCAAA
	Rev: ATCCCAGCACAGTCGATGAT
Traf6	For: TGTTGGATCCAGGAAATGTG
	Rev: GGCAGAAGTTGCTACAAGCAG
Nfkb	For: ACCCAAGGACATGGTGGTT
	Rev: CCCCTAATACACGCCTCTGT
Trem2	For: CGAGGAGTCATCGAGTTTCG
	Rev: AGGAGGAGAAGAATGGAGGTG
Dcstamp	For: CGCTGTGGACTATCTGCTGTA
	Rev: CCTTGGGTTCCTTGCTTCT
Ocstamp	For: TTGCTCCTGTCCTACAGTGC
	Rev: GCCCTCAGTAACACAGCTCA
Cd47	For: GCGATGCCATGGTGGGAAAC
	Rev: GAAAACCACGAAACCGTGCG
Synb	For: CCACCACCCATACGTTCAAA
	Rev: GGTTATAGCAGGTGCCGAAG
Atp6v0d2	For: AAGCCTTTGTTTGACGCTGT
	Rev: TGAATGCCAGCACATTCATC
Car2	For: TGAAGATTGGACCTGCCTCACA
	Rev: AGCAGAGGCGGAGTGGTCAG
Atp6v0d1	For: CCTGTGGTGCTGGCTGAAGACT
	Rev: GACACTGAGGGTTGATTGGCTGAC
Ctsk	For: GCAGGGTCCCAGACTCCATCG
	Rev: GCTGAAAGCCCAACAGGAACCAC
Acp5 (TRAP)	For: ATTTGTGGCTGTGGGCGACT
	Rev: GCACGGTTCTGGCGATCTCT
Spp1 (OPN)	For: GAGAGCCAGGAGAGTGCCCA
	Rev: GCTTTGGAACTTGCTTGACTATCG
Arg1	For: ATGACGTGAGAGACCACGGG
	Rev: TGCTTCCAACTGCCAGACTGT
Cdc6	For: ACACACTGTTTGAGTGGCCGT
	Rev: GCTTCAAGTCTCGGCAGAATTC
Ccnd1	For: AGTGCGTGCAGAAGGAGATT
	Rev: CACAACTTCTCGGCAGTCAA

2.9. Cathepsin K activity assay

Cathepsin K activity was measured in control and acidified osteoclasts using the fluorescent Cathepsin K Activity Assay kit (PromoCell, UK), as per the manufacturer's instructions. Cathepsin K activity was normalised to total protein to produce cathepsin K activity per μg of protein (relative fluorescence units, RFU/ml/μg protein).

2.10. TRAP activity assay

TRAP activity was measured using a modified protocol from an Acid Phosphatase Assay kit. Control and acidified osteoclasts were lysed in 0.1 % Triton® X-100 in PBS and cell lysates were incubated on ice for 10 min. Samples were vortexed for 5 min and centrifuged at 17,000 xg for 5 min at room temperature. The supernatant was transferred to a 96-well plate for protein quantification via the Bradford assay (BioRad, UK) and TRAP activity measurement. Acid phosphatase substrate buffer (0.5 M sodium acetate, 20 mg 4-nitrophenyl phosphate and 10 % sodium tartrate solution, pH 5.2) was added to the supernatant and incubated at 37 °C for 30 min. Cell-free lysis buffer with substrate buffer was negative control; acid phosphatase from potato (25 μg) was positive control; p-nitrophenol solution (5μmole/ml in 0.5 N NaOH) acted as a standard. Reactions were terminated by adding 0.5 N NaOH to all wells except the standard solution. Absorbance was measured at 405 nm.

2.11. High-resolution micro-computed tomography (μCT) scanning

Osteoclasts were cultured for 5 days at control or acidified pH. At this stage, discs were either fixed (0 h time point) or fully media changed and cultured for a further 24 h (24 h time point groups: control, acidified, switched). All fixed dentine discs with adherent osteoclasts were scanned using the Skyscan 1172 micro-CT scanner (Bruker, Belgium) at 40 kV and 250 μA with no filter and a voxel size of 2 μm. Resorption events on each slice were manually demarcated as the region of interest (CTAn). For morphometric analysis, images were binarized using a threshold range 0–60. Voxels with a greyscale value >60 become black (denoting background) and voxels <60 appear white (pores, i.e., resorption events). The percent bone volume/tissue volume (BV/TV) signified the percentage porosity (i.e., resorption volume) of the dentine disc. Resorption volume was normalised to the number of days exposed to pH treatment: 5–6 days for control and acidified osteoclasts and 1 day for switched osteoclasts. CTvox was used for visualisation of resorption pits.

2.12. RNA sequencing

Total RNA from control, acidified and switched osteoclasts 4-h post-acidification was extracted as described above. Polyadenylated transcript enrichment and strand specific library preparation was completed

using the NEBNext Ultra II mRNA kit (New England Biolabs, UK) following manufacturer's instructions. Sample quality control was performed using Qubit fluorometry (Invitrogen, UK) and the 2200 or 4200 TapeStation (Agilent, UK). RIN estimates for all samples were between 9.2 and 10. Paired-end sequencing was performed using a NovaSeq6000 platform (NovaSeq 6000 S2/S4 reagent kit v1.5, 300 cycles, Illumina, UK) and generated a raw read count of >25 million reads per sample. The expression of transcripts was quantified against the *Mus musculus* MM10 transcriptome using Salmon [30]. After exploratory analysis (e.g., mean-variance relationship, principal component analysis), differential gene expression analyses were conducted using the limma package [31]. A cut-off of a fold-change of 1.5 (linear space) and *p*-adjusted value ≤0.05 after correction for multiple testing using the Benjamini-Hochberg method was applied. The CAMERA function within the

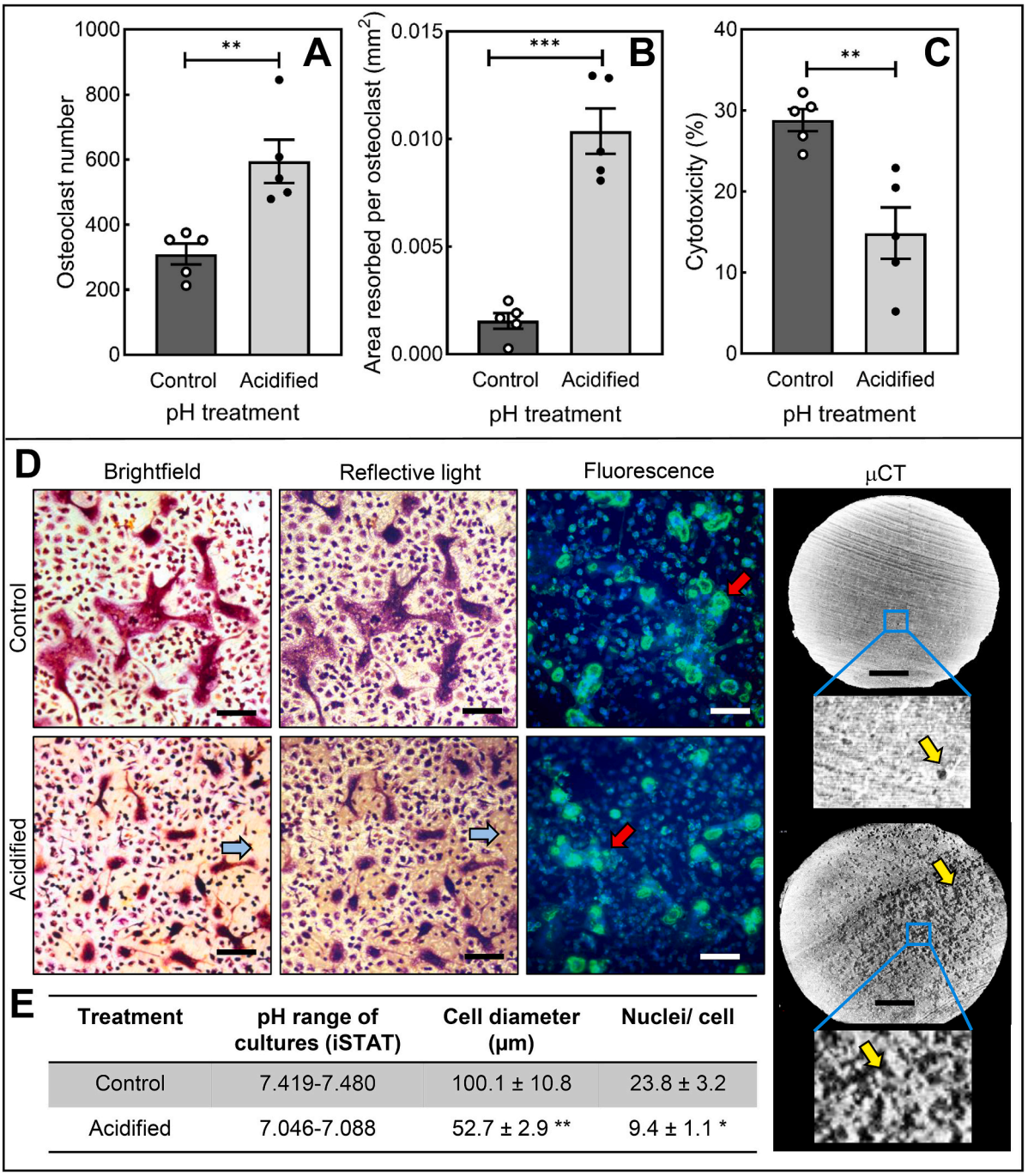

E

Treatment	pH range of cultures (iSTAT)	Cell diameter (µm)	Nuclei/ cell
Control	7.419-7.480	100.1 ± 10.8	23.8 ± 3.2
Acidified	7.046-7.088	52.7 ± 2.9 **	9.4 ± 1.1 *

Fig. 1. Extracellular pH regulates osteoclast number, size, activity and viability.
Culture at acidified pH (pH 7.0) increases (A) osteoclast number and (B) bone resorption and (C) reduces cytotoxicity compared to control (pH 7.4) conditions. (D) Brightfield and reflective light microscopy images showing the effect of pH on osteoclast formation and bone resorption (resorption pits are the tan areas illustrated by the light blue arrow). Fluorescence images illustrating the increased number of nuclei in control osteoclasts (highlighted by the red arrow): nuclei are stained with DAPI (blue) and the actin ring with phalloidin (green). µCT of entire discs shows extensive resorption (grey areas, highlighted by yellow arrows) in acidified cultures and the limited resorption in control cultures. Scale bars: microscopy = 200 µm, µCT = 0.9 mm. (E) Osteoclast diameter and nuclei number were reduced in acidified cultures compared to control cells. Data presented as mean ± SEM, n = 3–5 biological replicates as illustrated by individual points: * = $p < 0.05$, ** = $p < 0.01$, *** = $p < 0.001$. (For interpretation of the references to color in this figure legend, the reader is referred to the web version of this article.)

limma package determined the enriched functions of differentially expressed genes (DEGs) [32]. C2 Reactome curated gene sets comprising of 1604 gene sets were used to identify canonical pathways associated with DEGs [33,34]. Results with a false discovery rate (FDR) threshold of <0.05 were considered significant. Gene Set Variation Analysis (GSVA) estimated specific pathway activities over sample populations [35].

2.13. Statistics

All data were presented and analysed using GraphPad Prism v9.3.1 (San Diego, USA). Data are presented as bar graphs with points to show values for individual experiments or line graphs. In vitro results show data from 3 to 5 individual experiments; each experiment was performed using osteoclasts isolated from different animals. Within each experiment, each group contained 3–8 technical replicates (dentine discs). Data was analysed using a two-tailed *t*-test or randomised block ANOVA with Fisher's LSD *post-hoc* analysis as appropriate [36].

3. Results

3.1. Extracellular pH regulates osteoclast number, activity, size, multinucleation and cytotoxicity

Under acidified conditions (pH 7.0), the number of osteoclasts formed and their resorptive activity was 1.9-fold and 6.7-fold higher, respectively, than in control cultures (maintained at a physiologically neutral pH 7.4) (Fig. 1A, B & D). High resolution μCT images of the dentine disc show extensive resorption at an acidic pH and the limited resorption in control cultures (Fig. 1D). Cytotoxicity was reduced by 49 % in acidified osteoclasts (Fig. 1C). The cell diameter was 48 % smaller and the number of nuclei 60 % lower in actively resorbing, acidified osteoclasts compared to control cells (Fig. 1D–E). Representative brightfield, reflective and fluorescence images in Fig. 1D show the increased size, nuclei number and impaired resorption of control osteoclasts. The pH range of the medium in acidified and control cultures is shown in Fig. 1E.

3.2. pH regulates gene expression in mature osteoclasts

The effect of pH on the expression of osteoclast-associated genes was investigated using RT-qPCR. When compared to the mRNA levels in control cells, analysis revealed that expression of key genes associated with formation (*Nfatc1*, *Tnfrs11a* (RANK), *Csf1r*, *Traf6*) was higher in acidified osteoclasts (Fig. 2A). Increased expression of fusion (*Dcstamp*) and resorption-associated (*Ctsk*, *Atp6v0d2*, *Atp6v0d1*, *Spp1*) genes was also observed in acidified cells (Fig. 2B & C). *Nfkb*, *Synb*, *Car2* and *Acp5 all* displayed a trend towards increased mRNA expression in acidified osteoclasts (Fig. 2); however, considerable variation between biological replicates meant that this was not statistically significant.

3.3. Control osteoclasts express more DC-STAMP, cleaved OPN and cathepsin K protein

Representative western blots show decreased expression of DC-STAMP, MMP-cleaved OPN and cathepsin K in acidified osteoclasts compared to control cells; densitometry analysis revealed that levels of these proteins were reduced by up to 37 % (Fig. 3A & B). OPN and CAII protein expression was unaffected by pH treatment (Fig. 3A & \B). Cathepsin K enzyme activity was 2.2-fold greater in actively resorbing, acidified osteoclasts compared to resorption-limited control cells (p = 0.0823, Fig. 3C). TRAP activity was unaffected by extracellular pH (Fig. 3D).

3.4. Osteoclast size decreases and osteoclast number, resorptive activity and viability increases upon acid-activation

When compared to control cells, short-term exposure of mature osteoclasts to acidified conditions (termed “switched”) increased osteoclast number 1.6-fold and 2.1-fold within 8- and 24-h, respectively (Fig. 4A & F). Within 4-h of acidification, osteoclast diameter decreased by ~32 % relative to control and by 8 h was comparable to cells continually cultured in acidified conditions (Fig. 4B). Resorptive activity was visible in switched cells within 8-h, and by 24-h, resorption (both total and per osteoclast) was similar to acidified osteoclasts (Fig. 4C, D & F). Cytotoxicity in switched cells was ~52 % lower than control osteoclasts. There was no difference in cytotoxicity between acidified and

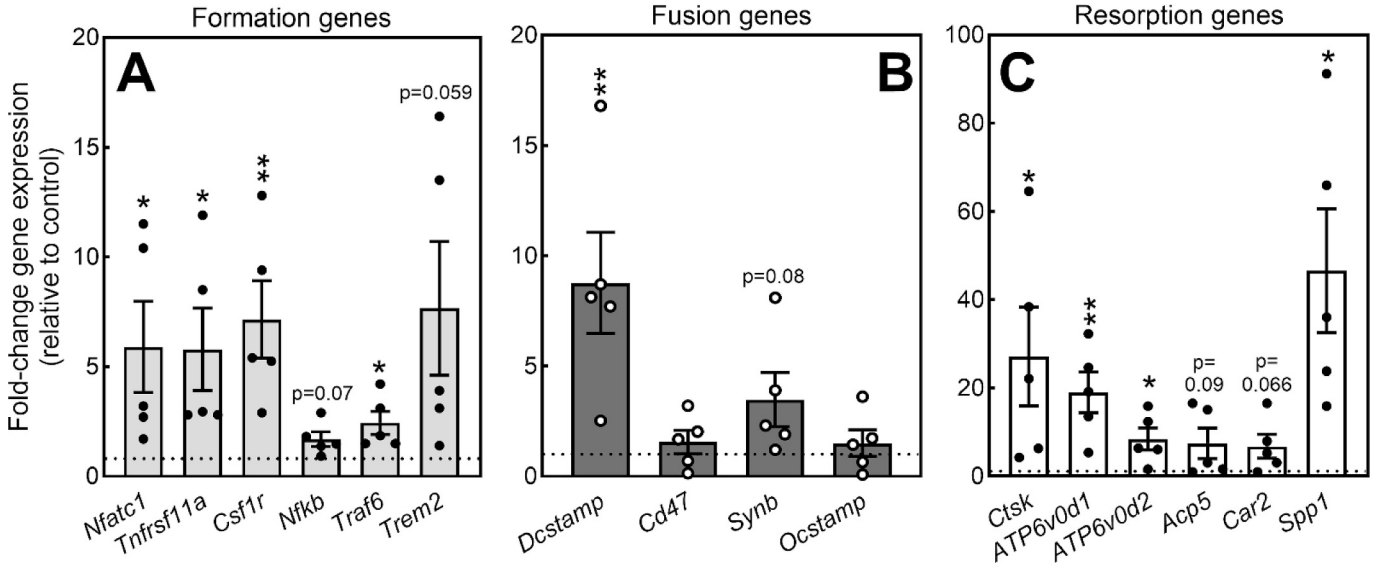

Fig. 2. The expression of genes involved in osteoclast formation and resorptive activity is increased in acidified osteoclasts.
Comparison of gene expression in acidified osteoclasts relative to control osteoclasts revealed significant changes in mRNA levels. Genes associated with (A) osteoclast formation (*Nfatc1*, *Tnfrs11a*, *Csf1r*, *Traf6*), (B) fusion (*Dcstamp*) and (C) bone resorption (*Ctsk*, *Atp6v0d2*, *Atp6v0d1*, *Spp1*) were increased in acidified osteoclasts. Data are normalised to TBP expression and presented as relative to control osteoclasts (shown by the dotted line). Data presented as mean ± SEM, n = 5 independent RNA sets as illustrated by individual points:* = p<0.05, ** = p < 0.01.

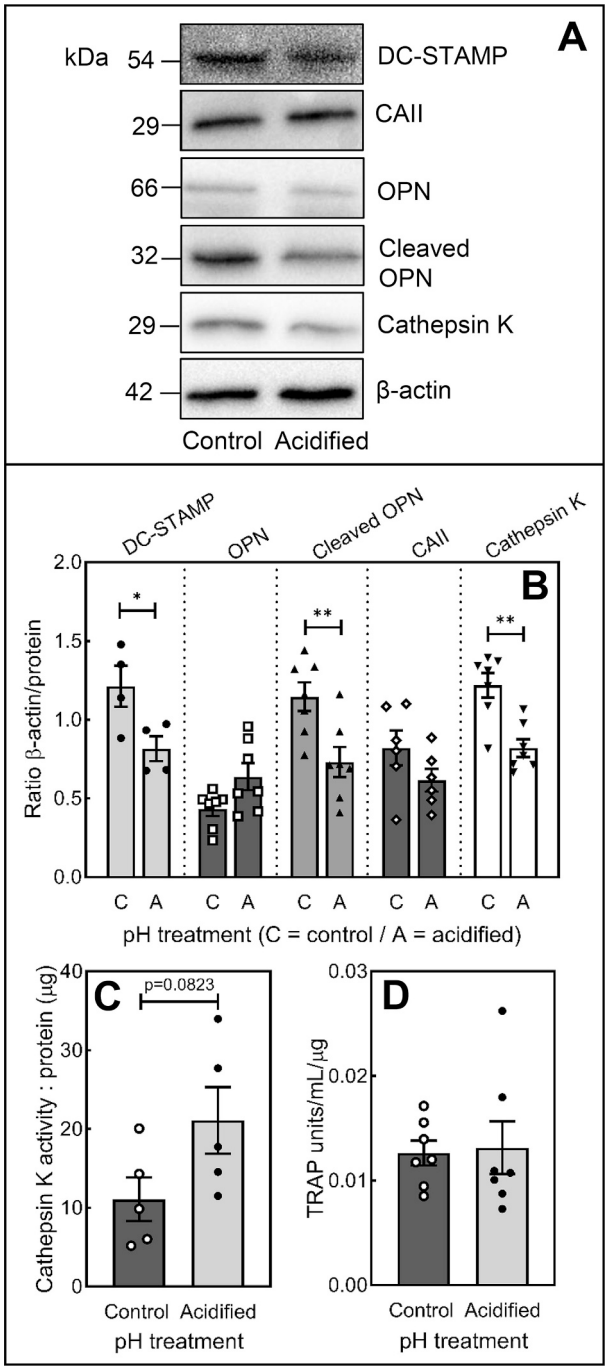

Fig. 3. Extracellular pH modulates the expression of osteoclast fusion and resorption-associated proteins.
(A) Representative western blots show that protein expression of DC-STAMP, cleaved OPN and cathepsin K was decreased in acidified osteoclasts relative to control cells: CAII and OPN were unchanged. (B) Densitometry analysis revealed protein levels of DC-STAMP, cleaved OPN and cathepsin K were up to 37 % lower in acidified osteoclasts. (C) Acidified osteoclasts show a trend towards greater cathepsin K activity compared to resorption limited control cells. (D) TRAP activity was unaffected by extracellular pH. Data shown as mean ± SEM, protein n = 4–7, all other data n = 5–6 biological replicates as illustrated by individual points, * = $p < 0.05$, ** = $p < 0.01$.

switched osteoclasts from 4-h post-acidification (Fig. 4E). Representative reflective light images of the changes in osteoclast size and increase in resorption in switched cells over 24 h are shown in Fig. 4F and a schematic of the experimental set up is shown in Fig. 4G.

Osteoclasts continually cultured under control conditions were consistent in number and size throughout the 24-h period (Fig. 4A, B & F). Resorptive activity was limited during the first 8 h then increased slightly (Fig. 4C & D). Whilst pit formation was observed in control cultures by 24-h, resorption remained significantly higher in acidified osteoclasts (either continually or short term) (Fig. 4C, D & F). Osteoclasts continually cultured in acidified conditions were consistent in size, number and resorptive activity and significantly different to control osteoclasts throughout (Fig. 4).

3.5. *The osteoclast transcriptome is modulated by small changes in extracellular pH*

The effect of pH on the osteoclast transcriptome was investigated in control, acidified and switched (acidified pH for 4 h) osteoclasts; see Fig. 4F for schematic of experimental set up. The gene expression profile of osteoclasts in each group clustered separately (Fig. S1). In terms of differentially expressed genes (DEGs), there were 499 up-regulated and 509 down-regulated in control osteoclasts compared to acidified cells (Fig. 5A & C). For control versus switched osteoclasts, there were 358 DEGs increased and 406 decreased in control cells (Fig. 5A & D). Finally, when comparing switched osteoclasts to those acidified throughout, 124 DEGs were up-regulated and 138 were down-regulated in the switched cells (Fig. 5A & E). Between the different comparisons, there was significant overlap in the genes found to be differentially expressed (Fig. 5B). For example, 184 genes were downregulated and 220 were upregulated, in control osteoclasts when compared to both acidified and switched cells (Fig. 5B). The expression of selected DEGs (*Arg1*, *Cdc6*, *Ccnd1*) was investigated by RT-qPCR using both new RNA samples as well as those used for the RNASeq (Fig. 5F). For all three genes, the PCR analysis displayed the same effect on gene expression as the RNASeq; for example, *Arg1*, *Cdc6*, *Ccnd1* expression were all decreased in control cells relative to acidic osteoclasts or in control cells relative to switched cells (Fig. 5F).

Table 2 summarises the functional analysis pathways associated with the DEGs. Metabolism-associated genes were commonly differentially expressed across all pH treatments. Energy metabolism (e.g., *Pck2*, *Nt5e*, *Arg1*, *Ido1*) and amino acid transport (e.g., *Slc6a12*, *Slc7a2*) were downregulated in control osteoclasts compared to both acidified and switched osteoclasts. Cell cycle-associated genes (*Cdc6*, *Ccnd1*, *Cenpk*) were also decreased in control osteoclasts. A three-way GSVA of metabolic pathways showed greater enrichment of protein synthesis pathways in switched osteoclasts compared to those continually cultured at control or acidified pH (Fig. 5G).

3.6. *Switched osteoclasts display higher levels of resorption*

Commonly used image analysis techniques can only determine the area of resorption not the depth/volume [27]. Therefore, µCT scanning was used to calculate both the number of resorption pits and the volume of resorption. Analysis of resorption was performed in control and acidified osteoclasts after 5 days of culture (0 h) and 24 h later in control, switched and acidified cells. At 0 and 24 h, little resorption was present in control cultures, whilst numerous resorption pits were evident in acidified osteoclasts. Switched cultures changed from displaying minimal resorption at 0 h to widespread resorptive activity at 24 h (see representative µCT images in Fig. 6A).

To show how active the osteoclasts were in the different conditions, µCT data were normalised to days in culture. Switched osteoclasts displayed a 24-fold and 6-fold increase in the number of resorption pits formed per day compared to control and acidified osteoclasts, respectively (Fig. 6A & B). The total volume resorbed showed a clear trend towards an increase in switched osteoclasts compared to control and acidified osteoclasts being 23-fold and 6.4-fold higher, respectively. However, this did not reach statistical significance (Fig. 6A & C).

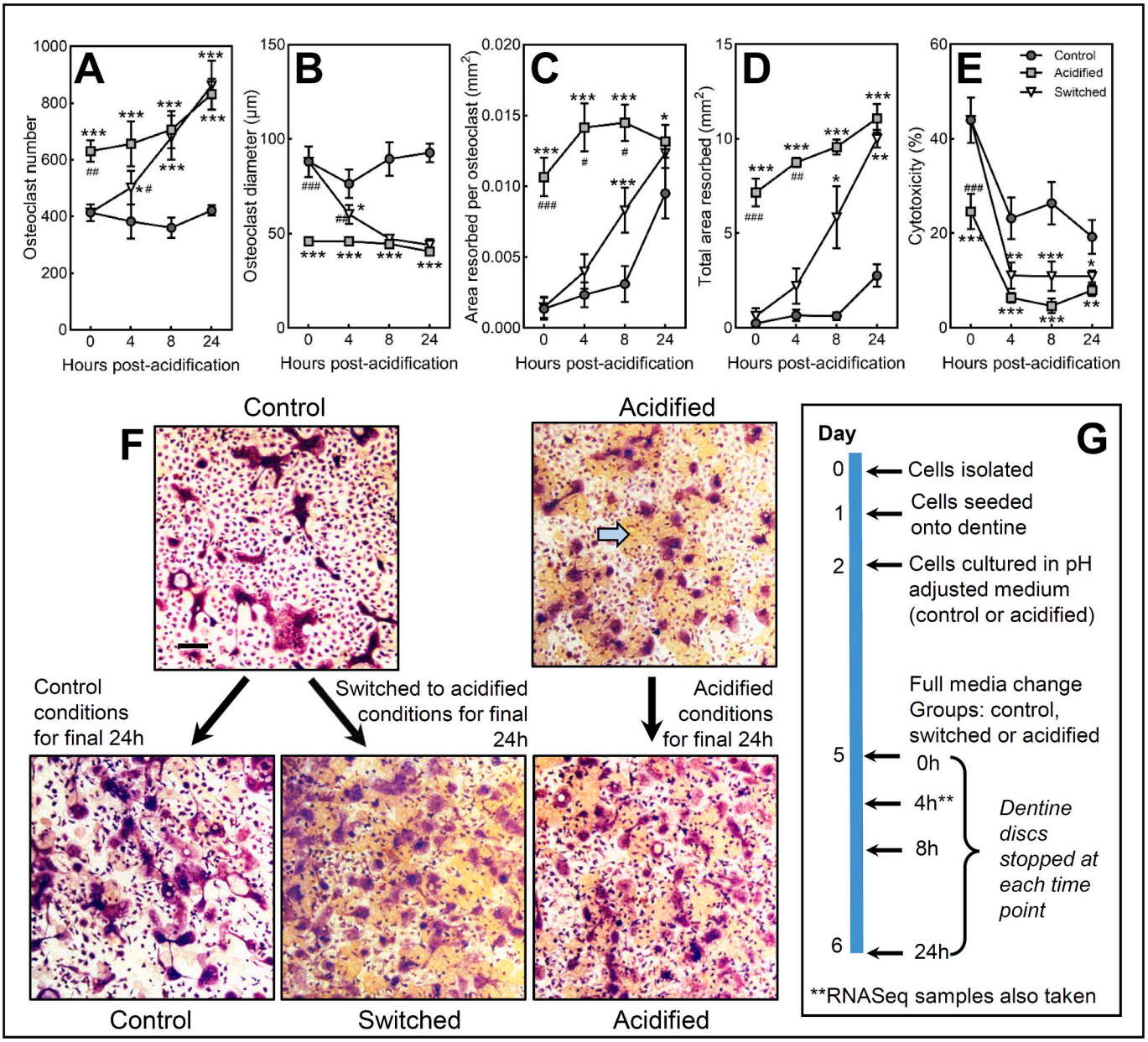

Fig. 4. Exposure of mature osteoclasts to acidified pH for 24 hour increases osteoclast number, and resorptive activity but reduces cell size.
After 5 days cultured at either control or acidified pH, osteoclasts were fully media changed and either maintained in these conditions or changed from control to acidified pH (termed switched) for up to 24 h. This short-term acidification of mature osteoclasts (A) increased osteoclast number and (B) reduced osteoclast diameter compared to control cells. At 0 h, switched osteoclasts displayed limited resorption but by 24 h, resorption levels (C) per osteoclast and (D) in total had increased and were comparable to acidified osteoclasts. (E) Switched and acidified osteoclasts displayed reduced cytotoxicity compared to control cells. Data presented at mean ± SEM, n = 5 biological replicates, * = $p < 0.05$, ** = $p < 0.01$. *** = $p < 0.001$. Asterisks (*) alone are differences between acidified or switched cells compared to control osteoclasts with each time point, # = difference between acidified and switched osteoclasts. (F) Reflective light microscopy images of control, acidified and switched osteoclasts at baseline (0 h) and after 24 h. Scale bar: 200 μm. (G) Schematic diagram showing the experimental set up for the short-term pH experiments.

4. Discussion

This study demonstrates that extracellular pH modulates osteoclast fusion, size and activity as well as the cell transcriptome. We observed that mouse osteoclasts generated in control conditions at 'physiological' pH (7.42–7.48) were large and highly nucleated but showed only limited resorption capacity. In contrast, osteoclasts cultured in acidified media (pH 7.05–7.09) were significantly smaller and had half the number of nuclei but were twice as abundant and exhibited 7-fold greater resorptive activity. When mature osteoclasts formed under control conditions were switched to acidified media, cell size reduced whilst number and resorptive activity increased reaching levels similar to those seen in continually acidified osteoclasts. These changes in morphology and activity occurred within a 24-h period. Osteoclast viability was also markedly improved in acidified media. Furthermore, several different genes and associated pathways, particularly metabolic pathways, were differentially regulated by extracellular pH. These data indicate that extracellular pH controls the "off/on" mechanisms that switch osteoclasts between fusion and active resorption modes eliciting significant morphological, phenotypic and transcriptomic effects on osteoclasts in as little as 4 h.

Consistent with the morphological findings, protein expression of DC-STAMP, regarded as a 'master fusogen', was lower in the smaller acidified osteoclasts compared to the larger control osteoclasts. In

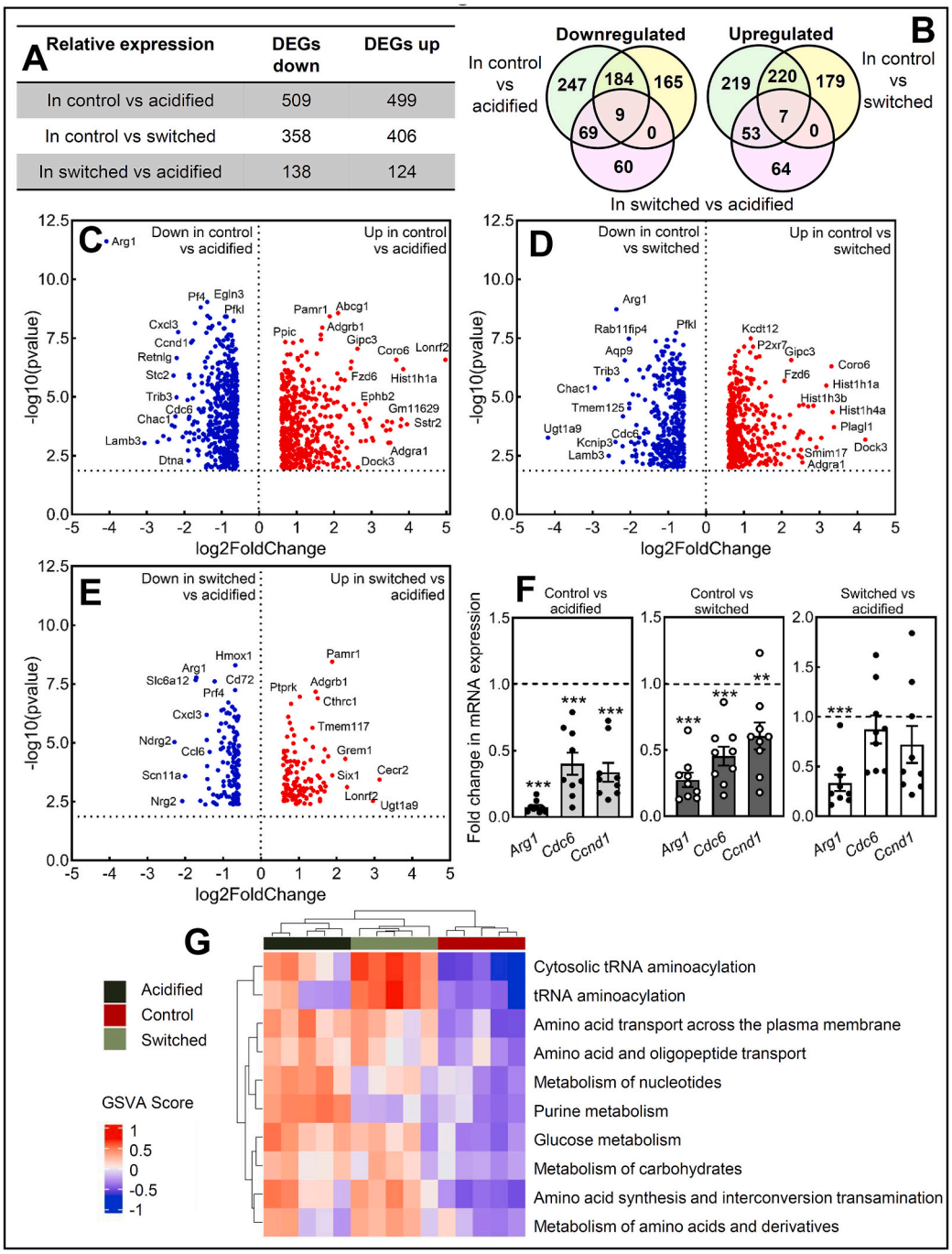

Fig. 5. An acidified pH induces significant changes in the osteoclast transcriptome.
RNASeq analysis was performed on mature osteoclasts (n = 5 biological replicates) cultured in control, acidified or switched (acidified pH for 4 h) conditions. (A) Summary of the numbers of differentially expressed genes (DEGs) and (B) Venn diagrams showing the overlap in DEGs between the different comparisons. Volcano plots showing the upregulated (red) and downregulated (blue) DEGs in osteoclasts cultured in (C) control vs acidified, (D) control vs switched and (E) switched vs acidified conditions (FDR < 0.05). Genes displaying the greatest fold change in expression are annotated. (F) Independent RT-qPCR analysis of selected DEGs shows *Arg1*, *Cdc6* and *Ccnd1* gene expression is reduced in control osteoclasts compared to both acidic and switched cells. Data shown as mean ± SEM, n = 8 independent RNA sets, ** = $p < 0.01$, *** = $p < 0.001$. (G) Gene set variation analysis (GSVA) of metabolism-associated pathways reveals greater enrichment of protein synthesis pathways in switched osteoclasts compared to control or acidified cells. (For interpretation of the references to color in this figure legend, the reader is referred to the web version of this article.)

contrast, *Dcstamp* mRNA levels were increased in acidified cells. This discrepancy was surprising given the striking trophic effects of acidic media on cell size but could reflect the common apparent disconnection between changes in mRNA and protein levels. Previous studies have reported that DC-STAMP is expressed early in osteoclastogenesis for cell fusion [37,38]. It is possible that early, transient changes in mRNA levels for this gene was missed in this study because gene expression analysis was conducted at day 5, by which time mature osteoclasts had already formed.

Our findings describing the effects of pH on osteoclast size contrast with other reports [25,26,39,40]. For example, Kato et al reported the formation of large TRAP+ multinucleated cells from mouse marrow at

Table 2
Differentially expressed genes and functional pathways in osteoclasts upon exposure to different extracellular pH treatments.

Comparison	Pathway	Differentially expressed genes (DEGs)
Upregulated in control vs. acidified	Regulation of Kit signalling	*Kitlg*, *Yes1*
	Serotonin receptors	*Htr1b*
	Regulation of Rheb GTPase activity by AMPK	*Prkaa2*
Downregulated in control vs. acidified	Amino acid synthesis, transport and metabolism	*Arg1*, *Phgdh*, *Slc6a12*, *Slc7a2*, *Ido2*, *Haao*, *Gatm*
	Cell cycle	*Cdc6*, *Ccnd1*, *Cenpk*
Downregulated in control vs. switched	Amino acid synthesis, transport and metabolism	*Arg1*, *Phgdh*, *Haao*, *Ido 1*, *Ido2*, *Cth*, *Kmo*, *Slc7a5*, *Slc1a4*, *Slc7a1*
	Glucose and protein metabolism	*Galnt15*, *Pck2*
Downregulated in switched vs. acidified	Immune signalling	*Peli3*
	Peptide ligand binding receptors	*Prokr2*
	Biological oxidations	*Ggt1*

low pH, whereas continued culture at pH ~7.4 formed few osteoclasts [25,26]. However, this work used osteoclasts co-cultured with an osteoblast-like cell line on plastic. These major methodological differences, including the substrate used to culture cells and the confounding effects of another cell type, makes direct comparisons between these studies and our own work difficult. Work by Muzylak et al. [22] showed that in long term cultures of cat peripheral blood mononuclear cells on dentine, the formation of giant osteoclasts and resorption pits was maximal at pH 7.0, a contrasting result that might reflect species differences. Our findings are also at variance with an early study that reported osteoclast nuclei number positively correlates with resorptive activity [40].

The activation of osteoclastic resorption at low pH observed here is clearly in line with earlier work [16,18,26,41]. Consistent with the increased resorption pit formation observed, mRNA expression of *Ctsk* and 2 subunits of the vATPase (*ATP6v0d1*, *ATP6v0d2*) was up-regulated in acidified osteoclasts relative to control cells; *Acp5* and *Car2* showed a trend to increased expression, but this did not reach statistical significance. The vATPase contributes to bone degradation by pumping H^+ across the ruffled border and acidifying the resorption pit [10]. Therefore, increased vATPase levels could promote resorption by enhancing matrix demineralisation when osteoclasts are in an acidified environment. Since the vATPase is a multi-subunit protein complex analysis of the different subunit protein levels or use of pharmacological inhibitors would be required to confirm this potential mechanism. Cathepsin K is one of the proteases responsible for matrix degradation. Whilst levels of cathepsin K protein were lower in acidified cells compared to control, overall enzyme activity showed a trend towards increased activity. This suggests that higher cathepsin K activity could also be contributing to the increased resorption seen in acidic cells. Together, these observations reinforce the concept that an acidic pH promotes resorption whereas a physiologically neutral extracellular pH results in limited osteoclast resorptive activity.

Previous work has reported that mature osteoclasts can undergo cell fission [42,43]. Fissioned osteoclasts, recently termed 'osteomorphs', are reported to be a transcriptionally distinct cell type which are capable of fusing, or recycling, to form functional osteoclasts upon administration of soluble RANKL [43]. The data presented suggest that osteoclast fission could be triggered by a reduction in extracellular pH. This hypothesis would explain the increased osteoclast numbers observed in the switched cultures within 4 h of acidification. However, further work (e.g., including live cell imaging) is required to validate this theory and establish the mechanisms involved.

Regarding changes in osteoclast function, switching control osteoclasts to a lower pH progressively increased resorptive activity over 24 h. In fact, switched osteoclasts resorbed as much bone substrate in 24 h as the continually acidified osteoclasts resorbed throughout the whole culture (6 days). These findings suggest that control osteoclasts, once activated by a reduction in pH, are capable of rapid, extensive and potentially more aggressive resorption compared to osteoclasts continually formed under acidified conditions. The molecular mechanisms underpinning these effects remain to be established, however, one potential candidate which is associated with resorption aggression is cathepsin K [44]. Together, our findings raise the interesting possibility that the environment in which osteoclasts are formed (e.g. pathological versus physiological) may directly influence resorption capacity once activated by the appropriate cellular signals.

RNAseq analysis was performed to investigate the effects of extracellular pH on the transcriptomic profile of osteoclasts. Comparison of control and acidified osteoclasts revealed that a total of 1008 genes were differentially expressed, highlighting the importance of pH in regulating osteoclast formation and activity. These DEGs were associated with processes including extracellular signalling, metabolism and the cell cycle. After 4 h exposure to acidified media, the gene expression profile of pH switched osteoclasts was closer to cells continually cultured at acidified pH, with only 262 DEGs identified. This reinforces the notion that osteoclasts can rapidly detect and rapidly respond to extracellular acidification to switch to their activated phenotype.

The observation that genes associated with the cell cycle were differentially expressed was surprising given that mature osteoclasts are formed by fusion. The reason behind this finding is unclear; it could be attributed to the actively dividing pre-osteoclasts which form part of the mixed cell population present in osteoclast cultures. Alternatively, it could indicate a role for these genes in driving the increased osteoclast number seen following a decrease in extracellular pH. Further work, including single cell approaches, would be required to fully investigate these hypotheses. Functional analysis also revealed that metabolic pathways including amino acid (e.g., *Arg1*, *Ido2*) and glucose metabolism and transport pathway gene sets, were enriched in osteoclasts exposed to low pH, irrespective of exposure duration, relative to control cells. The role of energy metabolism in osteoclasts and its impact on bone remodelling in health and disease is an important emerging area of research [45,46]. It is now apparent that the method via which osteoclasts generate energy changes according to differentiation stage [46]. In particular, bone resorption is an active, energy-consuming process requiring aerobic glycolysis and amino acid transport [46,47]. Therefore, the differential expression of these metabolic genes in actively resorbing cells compared to resorption-limited control osteoclasts is likely a biochemical response to meet the energetic and biosynthetic demands of bone resorption.

The findings presented here used osteoclasts derived from males and females in combination, the only exception being the RNASeq analysis which was performed on osteoclasts derived from females only. Whether the effects of extracellular acidification on osteoclast function differ between males and females was not examined here but represents an area for future study. A recent study demonstrated that male and female osteoclasts derived from conditional gremlin-1 knockouts displayed differential effects on formation and resorption in vitro [48]. This suggests that intrinsic sex-dependent effects on osteoclasts are indeed evident in cells generated in an artificial in vitro environment with excess levels of M-CSF and RANKL.

In conclusion, our findings reveal these a hitherto unknown effect of extracellular pH on osteoclasts and identify gene products and pathways associated with the rapid response to acidification. In addition to its

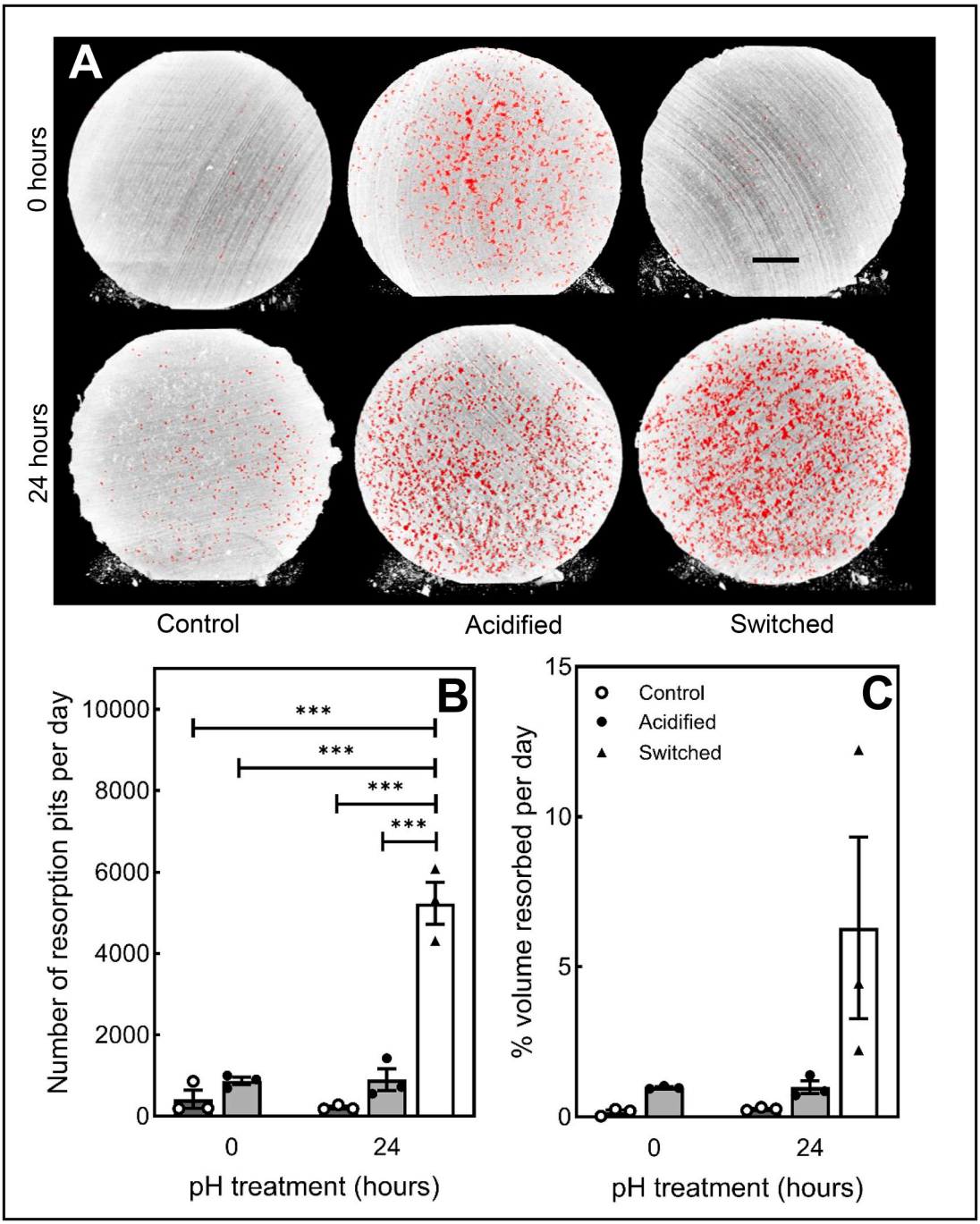

Fig. 6. Switched osteoclasts display an increased capacity to resorb.
(A) Analysis of bone resorption by μCT revealed that the number of resorption pits formed (when normalised for time exposed to the pH treatment) was increased 24-fold and 6-fold in switched compared to control and acidified cultures, respectively. (B) The volume of resorption was 23-fold and 6.4-fold higher in switched cells relative to control and acidified osteoclasts, respectively. Data presented as mean ± SEM, n = 3 biological replicates as illustrated by individual points, *** = $p < 0.001$. (C) μCT images showing the effect of short-term pH reduction on resorption pit formation 24 h post-acidification. Red shading denotes the resorption events quantified. Scale bar = 0.9 mm. (For interpretation of the references to color in this figure legend, the reader is referred to the web version of this article.)

well-known action on resorption pit formation, extracellular pH is also a fundamental regulator of osteoclast fusion and size that switches cells between formation and resorptive activity. Our results suggest the possibility that the processes of osteoclast fusion and activation take place in distinct 'niches' within the bone. For example, the fusion of osteoclasts might be favoured in higher pH extracellular environments near the capillaries from which their myeloid precursors extravasate. Migration of newly formed multinucleated osteoclasts away from the microvasculature into adjacent environments that are less well perfused, and thus more acidic, would result in the cessation of fusion and activation of bone resorption. In addition to providing important clarifications regarding the optimal conditions for functional osteoclasts in vitro, these findings could provide insights into the regulation of osteoclast behaviour in bone loss disorders associated with pH or vascular disturbances, for example in renal disease, diabetes and ageing.

Supplementary data to this article can be found online at https://doi.org/10.1016/j.bone.2025.117466.

CRediT authorship contribution statement

Bethan K. Davies: Writing – review & editing, Writing – original draft, Visualization, Validation, Project administration, Methodology, Investigation, Formal analysis, Data curation, Conceptualization. **Andrew J. Skelton:** Writing – review & editing, Visualization, Validation, Methodology, Investigation, Formal analysis, Data curation. **Mark Hopkinson:** Writing – review & editing, Methodology. **Simon Lumb:** Resources, Methodology. **Gill Holdsworth:** Writing – review & editing, Supervision. **Timothy R. Arnett:** Writing – review & editing, Supervision. **Isabel R. Orriss:** Writing – review & editing, Visualization, Supervision, Project administration, Investigation, Funding acquisition, Formal analysis, Data curation, Conceptualization.

Declaration of competing interest

Bethan K Davies: I have nothing to declare.
Andrew J Skelton: Is an employee of UCB Pharma and holds stock/stock awards.
Mark Hopkinson: I have nothing to declare.
Simon Lumb: Is an employee of UCB Pharma and holds stock/stock awards.
Gill Holdsworth: Is an employee of UCB Pharma and holds stock/stock awards.
Timothy R Arnett: I have nothing to declare.
Isabel R Orriss: I have nothing to declare.

Acknowledgements

This project was funded by the Biotechnology and Biological Sciences Research Council (BBSRC) through the London Interdisciplinary Doctoral Programme and UCB Pharma Ltd. (grant ID: BB/M009513/1). The authors would also like to acknowledge Dr. Simon Engledow at the Oxford Genomics Centre for his assistance with the RNASeq.

Data availability

Data available on request from the authors.

References

[1] N. Takahashi, N. Udagawa, T. Suda, A new member of tumor necrosis factor ligand family, ODF/OPGL/TRANCE/RANKL, regulates osteoclast differentiation and function, Biochem. Biophys. Res. Commun. 256 (1999) 449–455.
[2] D.L. Lacey, E. Timms, H.L. Tan, M.J. Kelley, C.R. Dunstan, T. Burgess, et al., Osteoprotegerin ligand is a cytokine that regulates osteoclast differentiation and activation, Cell 93 (1998) 165–176.
[3] M. Asagiri, H. Takayanagi, The molecular understanding of osteoclast differentiation, Bone 40 (2007) 251–264.
[4] M. Yagi, T. Miyamoto, Y. Sawatani, K. Iwamoto, N. Hosogane, N. Fujita, et al., DC-STAMP is essential for cell-cell fusion in osteoclasts and foreign body giant cells, J. Exp. Med. 202 (2005) 345–351.
[5] M. Yang, M.J. Birnbaum, C.A. MacKay, A. Mason-Savas, B. Thompson, P.R. Odgren, Osteoclast stimulatory transmembrane protein (OC-STAMP), a novel protein induced by RANKL that promotes osteoclast differentiation, J. Cell. Physiol. 215 (2008) 497–505.
[6] A.M. Moller, J.M. Delaisse, K. Soe, Osteoclast Fusion: time-lapse reveals involvement of CD47 and syncytin-1 at different stages of nuclearity, J. Cell. Physiol. 232 (2017) 1396–1403.
[7] K. Soe, T.L. Andersen, A.S. Hobolt-Pedersen, B. Bjerregaard, L.I. Larsson, J. M. Delaisse, Involvement of human endogenous retroviral syncytin-1 in human osteoclast fusion, Bone 48 (2011) 837–846.
[8] S.H. Lee, J. Rho, D. Jeong, J.Y. Sul, T. Kim, N. Kim, et al., v-ATPase V0 subunit d2-deficient mice exhibit impaired osteoclast fusion and increased bone formation, Nat. Med. 12 (2006) 1403–1409.
[9] D.M. Biskobing, D. Fan, Acid pH increases carbonic anhydrase II and calcitonin receptor mRNA expression in mature osteoclasts, Calcif. Tissue Int. 67 (2000) 178–183.
[10] J.M. Kim, S.K. Min, H. Kim, H.K. Kang, S.Y. Jung, S.H. Lee, et al., Vacuolar-type H +-ATPase-mediated acidosis promotes in vitro osteoclastogenesis via modulation of cell migration, Int. J. Mol. Med. 19 (2007) 393–400.
[11] J. Lemann Jr., J.R. Litzow, E.J. Lennon, The effects of chronic acid loads in normal man: further evidence for the participation of bone mineral in the defense against chronic metabolic acidosis, J. Clin. Invest. 45 (1966) 1608–1614.
[12] D.A. Bushinsky, R.J. Lechleider, Mechanism of proton-induced bone calcium release: calcium carbonate-dissolution, Am. J. Phys. 253 (5 Pt 2) (1987) F998–1005.
[13] J.H. Dominguez, L.G. Raisz, Effects of changing hydrogen ion, carbonic acid, and bicarbonate concentrations on bone resorption in vitro, Calcif. Tissue Int. 29 (1) (1979) 7–13.
[14] D.A. Bushinsky, Net calcium efflux from live bone during chronic metabolic, but not respiratory, acidosis, Am. J. Phys. 256 (1989) F836–F842.
[15] D.A. Bushinsky, N.S. Krieger, D.I. Geisser, E.B. Grossman, F.L. Coe, Effects of pH on bone calcium and proton fluxes in vitro, Am. J. Phys. 245 (1983) F204–F209.
[16] T.R. Arnett, D.W. Dempster, Effect of pH on bone resorption by rat osteoclasts in vitro, Endocrinology 119 (1986) 119–124.
[17] T.R. Arnett, A. Boyde, S.J. Jones, M.L. Taylor, Effects of medium acidification by alteration of carbon dioxide or bicarbonate concentrations on the resorptive activity of rat osteoclasts, J. Bone Miner. Res. 9 (1994) 375–379.
[18] T.R. Arnett, M. Spowage, Modulation of the resorptive activity of rat osteoclasts by small changes in extracellular pH near the physiological range, Bone 18 (1996) 277–279.
[19] S. Meghji, M.S. Morrison, B. Henderson, T.R. Arnett, pH dependence of bone resorption: mouse calvarial osteoclasts are activated by acidosis, Am. J. Physiol. Endocrinol. Metab. 280 (2001) E112–E119.
[20] P. Goldhaber, L. Rabadjija, H+ stimulation of cell-mediated bone resorption in tissue culture, Am. J. Phys. 253 (1987) E90–E98.
[21] A. Teti, H.C. Blair, P. Schlesinger, M. Grano, A. Zambonin-Zallone, A.J. Kahn, et al., Extracellular protons acidify osteoclasts, reduce cytosolic calcium, and promote expression of cell-matrix attachment structures, J. Clin. Invest. 84 (1989) 773–780.
[22] M. Muzylak, T.R. Arnett, J.S. Price, M.A. Horton, The in vitro effect of pH on osteoclasts and bone resorption in the cat: implications for the pathogenesis of FORL, J. Cell. Physiol. 213 (2007) 144–150.
[23] T. Shibutani, J.N. Heersche, Effect of medium pH on osteoclast activity and osteoclast formation in cultures of dispersed rabbit osteoclasts, J. Bone Miner. Res. 8 (1993) 331–336.
[24] R.J. Murrills, L.S. Stein, D.W. Dempster, Stimulation of bone resorption and osteoclast clear zone formation by low pH: a time-course study, J. Cell. Physiol. 154 (1993) 511–518.
[25] K. Kato, M. Matsushita, Proton concentrations can be a major contributor to the modification of osteoclast and osteoblast differentiation, working independently of extracellular bicarbonate ions, J. Bone Miner. Metab. 32 (2014) 17–28.
[26] K. Kato, I. Morita, Acidosis environment promotes osteoclast formation by acting on the last phase of preosteoclast differentiation: a study to elucidate the action points of acidosis and search for putative target molecules, Eur. J. Pharmacol. 663 (2011) 27–39.
[27] I.R. Orriss, T.R. Arnett, Rodent osteoclast cultures. Methods Mol. Biol. 816 (2012) 103–117.
[28] B.K. Davies, A.P. Hibbert, S.J. Roberts, H.C. Roberts, J.C. Tickner, G. Holdsworth, et al., A machine learning-based image segmentation method to quantify in vitro osteoclast culture endpoints, Calcif. Tissue Int. 113 (2023) 437–448.
[29] K.J. Livak, T.D. Schmittgen, Analysis of relative gene expression data using real-time quantitative PCR and the 2(-Delta Delta C(T)) Method, Methods 25 (2001) 402–408.
[30] R. Patro, G. Duggal, M.I. Love, R.A. Irizarry, C. Kingsford, Salmon provides fast and bias-aware quantification of transcript expression, Nat. Methods 14 (2017) 417–419.
[31] M.E. Ritchie, B. Phipson, D. Wu, Y. Hu, C.W. Law, W. Shi, et al., limma powers differential expression analyses for RNA-sequencing and microarray studies, Nucleic Acids Res. 43 (2015) e47.
[32] D. Wu, G.K. Smyth, Camera: a competitive gene set test accounting for inter-gene correlation, Nucleic Acids Res. 40 (2012) e133.
[33] B. Jassal, L. Matthews, G. Viteri, C. Gong, P. Lorente, A. Fabregat, et al., The reactome pathway knowledgebase, Nucleic Acids Res. 48 (2020) D498–D503.
[34] A. Fabregat, K. Sidiropoulos, G. Viteri, O. Forner, P. Marin-Garcia, V. Arnau, et al., Reactome pathway analysis: a high-performance in-memory approach, BMC Bioinformatics. 18 (2017) 142.
[35] S. Hanzelmann, R. Castelo, J. Guinney, GSVA: gene set variation analysis for microarray and RNA-seq data, BMC Bioinformatics. 14 (2013) 7.
[36] M.F. Festing, Guidelines for the design and statistical analysis of experiments in papers submitted to ATLA, Altern. Lab. Anim 29 (2001) 427–446.
[37] A.S. Hobolt-Pedersen, J.M. Delaisse, K. Soe, Osteoclast fusion is based on heterogeneity between fusion partners, Calcif. Tissue Int. 95 (1) (2014) 73–82.
[38] A.E. Coudert, F. Redelsperger, Y. Chabbi-Achengli, C. Vernochet, C. Marty, X. Decrouy, et al., Role of the captured retroviral envelope syncytin-B gene in the fusion of osteoclast and giant cell precursors and in bone resorption, analyzed ex vivo and in vivo in syncytin-B knockout mice, Bone Rep. 11 (2019) 100214.
[39] R.L. Lees, V.K. Sabharwal, J.N. Heersche, Resorptive state and cell size influence intracellular pH regulation in rabbit osteoclasts cultured on collagen-hydroxyapatite films, Bone 28 (2001) 187–194.
[40] K. Piper, A. Boyde, S.J. Jones, The relationship between the number of nuclei of an osteoclast and its resorptive capability in vitro, Anat Embryol (Berl). 186 (1992) 291–299.
[41] T.R. Arnett, D.W. Dempster, A comparative study of disaggregated chick and rat osteoclasts in vitro: effects of calcitonin and prostaglandins, Endocrinology 120 (1987) 602–608.

[42] I.D. Jansen, J.A. Vermeer, V. Bloemen, J. Stap, V. Everts, Osteoclast fusion and fission, Calcif. Tissue Int. 90 (2012) 515–522.
[43] M.M. McDonald, W.H. Khoo, P.Y. Ng, Y. Xiao, J. Zamerli, P. Thatcher, et al., Osteoclasts recycle via osteomorphs during RANKL-stimulated bone resorption, Cell 184 (1330–47) (2021) e13.
[44] X.G. Borggaard, D.C. Pirapaharan, J.M. Delaisse, K. Soe, Osteoclasts' ability to generate trenches rather than pits depends on high levels of active cathepsin K and efficient clearance of resorption products, Int J Mol Sc. (2020) 21.
[45] T.R. Arnett, I.R. Orriss, Metabolic properties of the osteoclast, Bone 115 (2018) 25–30.
[46] M.G. Ledesma-Colunga, V. Passin, F. Lademann, L.C. Hofbauer, M. Rauner, Novel insights in osteoclast energy metabolism, Curr. Osteoporos. Rep. 21 (2023) 660–669.
[47] A.B.P. Ribet, P.Y. Ng, N.J. Pavlos, Membrane transport proteins in osteoclasts: the ins and uuts, Front. Cell Dev. Biol. 9 (2021) 644986.
[48] M.H.C. Sheng, C.H. Rundle, D.J. Baylink, K.H.W. Lau, Conditional deletion of gremlin-1 in cathepsin K-expressin mature osteoclasts altered the skeletal response to calcium depletion in sex-dependednt manner, Calcif. Tissue Int. 116 (2025) 28.